



A Comparative Three-Dimensional Study about the Effects of the Hot Gas Passages on a Sectional Cast-Iron Boiler Performance

Rahim Hassanzadeh*, Faraz Marami Mashoof, Mohsen Darvishyedegari

Department of the Mechanical Engineering, Urmia University of Technology, Urmia, Iran

***Corresponding Author:** *Rahim Hassanzadeh, Department of the Mechanical Engineering, Urmia University of Technology, Urmia, Iran*

Abstract: *In the present study, a comparative investigation has been performed on the impact of the hot gas passages on a sectional cast-iron boiler (CIB) performance. To this end, various shapes of the hot gas passages such as the circle (case-1), hexagon (case-2), square (case-3), vertical ellipse with constant aspect ratio (AR) of 2 (case-4), and horizontal ellipse with AR=2 (case-5), have been considered and compared with each other in order to find the best geometry among the cases under consideration. Computations are carried out at two water flow rates of 0.015 and 0.030 kg/s and a three-dimensional flow domain is designed based on the dimensions of a real CIB section. It is found that case-5 has the maximum heat transfer rate and goodness factor with the highest sensitivity to the water flow rate among all cases under consideration. It was hoped that the obtained results arouse interest among the boiler designers.*

Keywords: *Sectional Cast-Iron Boiler (CIB), Hot Gas Passages, Convective Heat Transfer*

1. INTRODUCTION

It is known that energy plays a central role in the development of the countries. Energy is an essential input for agricultural production, transportation, industry, and business and the economy of each country is strongly depended to energy usage. Although, the renewable energy technologies are developing all over the world, however, global fossil fuels consumptions increased in 2015 [1]. According the published statistics, oil is the world's leading fuel with 32.9% of global energy consumption in 2015 [1]. In addition, natural gas and coal are accounted for 23.8% and 29.2% of global primary energy consumptions in 2015 [1]. A general review in the published official reports shows that fossil fuels are still popular all over the world. In this situation, monitoring the air pollution and carbon emission is a great need for all countries in today's world. Undoubtedly, managing the fossil fuel consumption is one of the ways to control the carbon emission and air pollution. In this regard, all equipments which are the fossil fuel consumers should be improved to be energy efficient systems. Domestic sectional CIBs are the common heat sources which use for different applications. They are constructed in various forms for supporting the small and moderate thermal capacities. The old versions of CIBs were constructed in single-pass form. Nowadays, although the single-pass sectional CIBs are still produced, however, most of these boiler are in three-pass form. Construction of a sectional boiler in three-pass form allows to have specific output with lower fuel consumption in comparison to the conventional single-pass boilers.

Unfortunately, there are very restricted investigations on the domestic boilers in general and on the sectional CIBs in particular. Some of them are worth mentioning, for example, Leyssens et al. [2] examined cardboard/sawdust in a domestic boiler by using a commercial pellet boiler and revealed that pellets containing cardboard lead to very good combustion. The relation between the fuel quality and gaseous and particulate matter emissions in a domestic pellet-fired boiler was investigated by Garcia-Maraver et al. [3]. They reported several results; for example, with a similar nitrogen content, NO_x emissions from the cork and olive wood pellets were higher than those from the pine based pellets. Fernandes et al. [4] investigated the oxidation behavior particulate matter from a domestic pellet-fired boiler and indicated that the oxidation rate near the flame boundary is significantly less than that of near the burner axis. Dias et al. [5] conducted the effect of different pellet types on 13 kW commercial domestic boiler efficiency. They showed that unburned heat losses were higher for pellets with a mean diameter larger than the one recommended for the present boiler. Fernandes and Costa

[6] studied the particle emission from a domestic pellets-fired boiler during the steady-state operation for different boiler thermal inputs. They concluded that the particle emissions between the 160 and 490 mg/Nm³ were mainly dominated by particles having the sizes either less than 2.5 μm or larger than 10 μm. In another work regarding the pellet boilers, Rabaçal et al. [7] compared the combustion and emission characteristics of various pellets such as pine, industrial wood wastes, and peach stones. It was found that the pine type pellet has better emission characteristics than the others.

Regarding the other types of the boilers, Horak et al. [8] compared the old (over-fire boiler and boiler with down-draft combustion) and new (automatic boiler and gasification boilers) types of the hot water domestic boilers in terms of the polycyclic aromatic hydrocarbons emissions. De Paepe et al. [9] compared different testing methods in order to determine the efficiency of a gas-fired domestic boiler. They stated that the measurement of the temperature is critical to assess the boiler efficiency. Additionally, the secondary circuit measurements should be preferred in this regard. Buczyński et al. [10] presented a numerical work about the combustion improvement in the small-scale domestic boilers. For this goal, they applied a deflector for redirecting the supply air and a modified combustion chamber. Vignali [11] compared the condensing domestic boiler with traditional type using the life cycle methodology in different climates. The 23% lower environmental impact is achieved for condensing boiler in comparison to that of the traditional boiler. Keppel et al. [12] studied the cereal grain combustion in domestic boilers. They concluded that the combustion of oat grains at a moisture content of 15% compares favorably with wood pellet combustion, but the combustion of other cereal grains is more problematic and may require more specialized technology. Gómez et al. [13] used a thermally thick approach to simulate a commercial biomass domestic boiler. They reported that the authors' proposed model showed a slightly better behavior of the thermally thick approach in the predictions of temperatures and excess air coefficient in the fumes, similar results in the CO₂ emissions and lower average values and thinner ranges in CO emissions. Las-Heras-Casas et al. [14] conducted the biomass boilers application for heating and domestic hot water in multi-familiar buildings in Spain. A reduction of 93% in the primary non-renewable energy consumption and 94% reduction in CO₂ emissions are reported in their investigation.

In the numerical work presented by Hassanzadeh et al. [15], effects of the hot gas passages on the thermal performance of the sectional CIBs were investigated two-dimensionally. Several shapes such as the circle, square, horizontal ellipse, and vertical ellipse as the hot gas passage were compared with each other in the mass flow rates ranging from 0.2 to 0.5 kg/s. They found that sectional CIB with a square shape passage provides maximum energy performance among the cases under consideration. In a three-dimensional work, Hassanzadeh et al. [16] conducted on the heat transfer process in a sectional CIB with several types of the hot gas passages. They compared various shapes of the hot gas passages such as the circle, hexagon, square, and ellipse and concluded that the section equipped with a square hot gas passage provides the maximum heat transfer with a minimum pressure drop among the cases under consideration.

Examination of the previously published works in the open literature shows that effects of the hot gas passages on the thermal performance of the sectional CIBs with four passage at each left and right-hand side of the section have not been studied to date. Since the shape, size, and the number of the hot gas passages affect the sectional CIB performance, therefore, this paper discusses on the heat transfer process of the sectional CIB with four channels at each left and right-hand side.

2. PROBLEM DESCRIPTION AND NUMERICAL ANALYSIS

In this study, effects of the hot gas passages on the thermal performance of a three-pass sectional CIB are investigated, numerically. In order to have a clear sense about the single-pass and three-pass boilers, figures 1(a) and (b) are provided which show the corresponding flow diagrams, schematically. In a single-pass section, as illustrated in figure 1 (a), the gas-air mixture after the combustion process inside the combustion chamber, moves within the chamber toward the rear side of the boiler and exhausts to the atmosphere via the chimney. Therefore, the surfaces of the combustion chamber are the main heat exchange area between the water and hot gas flows. In such single-pass sections, due to a restriction in the heat transfer area, the exhausted hot gases have still high temperature and hence, the thermal performance of the CIBs made with single-pass sections are usually low. Several suggestions have been presented in order to enhance the thermal efficiency of the sectional CIBs. One of the most effective ways in this regard is the construction of the sections in a three-pass model.

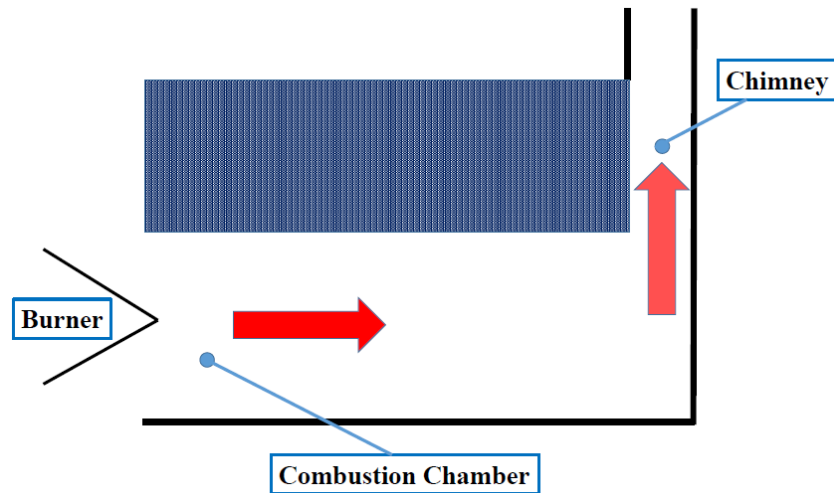


Figure1. Flow diagram of the sectional CIB; (a) single-pass

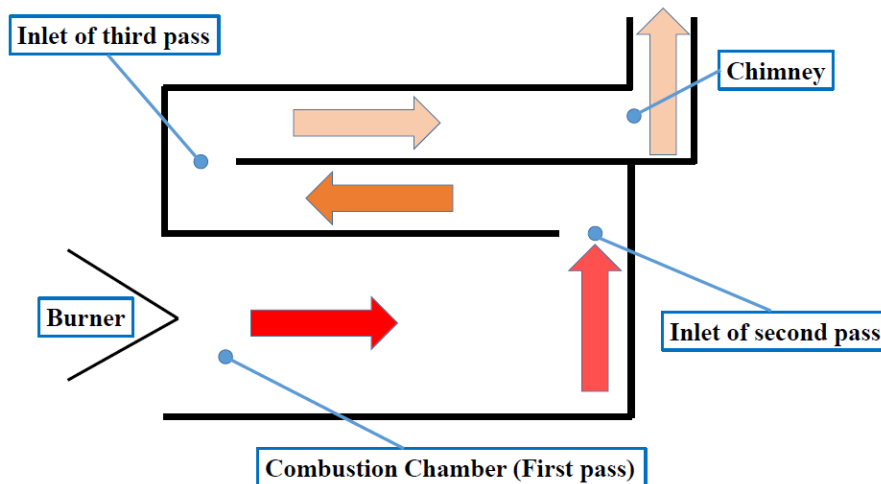


Figure1. Flow diagram of the sectional CIB; (b) three-pass

Figure 1(b) shows a hot gas flow schematic diagram for a three-pass sectional CIB. In a three-pass CIB, the gas-air mixture after a combustion process moves toward the rear side of the boiler within the combustion chamber called first pass, and then the hot gases turn toward the smaller channels and go through the one or a number of the passages toward the front side of the boiler which is called the second pass. The hot gases turn again toward the similar smaller channels and move along the boiler toward the rear side called third pass and finally exhaust to the atmosphere via chimney as shown in figure 1(b). Therefore, in addition to the surfaces of the combustion chamber, the surfaces of the second and third pass increase the hot gas-water total heat transfer area. Moreover, the retention time of the hot gases within the boiler extends using the multi-pass sections which is a useful parameter in the heat transfer process.

There are some important challenges in designing the three-pass sections. The first one is the shape of the second and third passages which is an important parameter. The shape of these passages affects the heat transfer rate of the boiler since the interaction level between the water flow and hot gas passages depends on the shape of these passages. On the other hand, the number of these passages at each right and left-hand side of the section is the other effective parameter. Some manufacturers use a single channel at each side of the section as the second and third passes whereas, some others, use two, three or four passages for this purpose. Hence, both the shape and number of the hot gas passages are depended on the manufacturer's strategy. For instance, two various section models are demonstrated in figure 2 in which in the right-hand side model, two passages in two rows are designed for second and third passes while in the left-hand side model, four passages in two rows are embedded for this issue. The under consideration domain in the present study is highlighted in figure 2 which covers the second and third pass area.

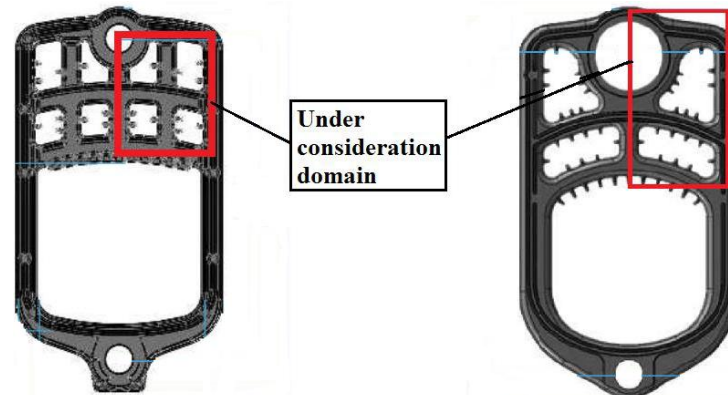


Figure2. Samples of the three-pass section and the under consideration domain in the present study denoted by red line

In order to model the section, a three-dimensional physical domain as figure 3 is designed in the present study according to a real section model. The constructed domain consists of a rectangle with four hot gas channels in which the vertical and horizontal free spaces between the channels are identical and twice of the free-space between the channels and corresponding side walls. Due to the symmetry condition between the left and right-hand side of the section, only the half of the section is analyzed in the present study. The first row (s_1 and s_2) and second row (t_1 and t_2) of the hot gas passages indicate the second pass and third pass, respectively. Therefore, two passages for the second pass and two passages for the third pass are considered at each side of the section. The water flow injects to the section via a small rectangular section located on the lower wall very close to the right wall and exits the channel via a semi-circular surface at the conjunction of the upper wall and symmetric plane. All necessary dimensions are indicated in table 1 in non-dimensional form. It should be said that all dimensions regarding the under consideration section are based on a real section in practice.

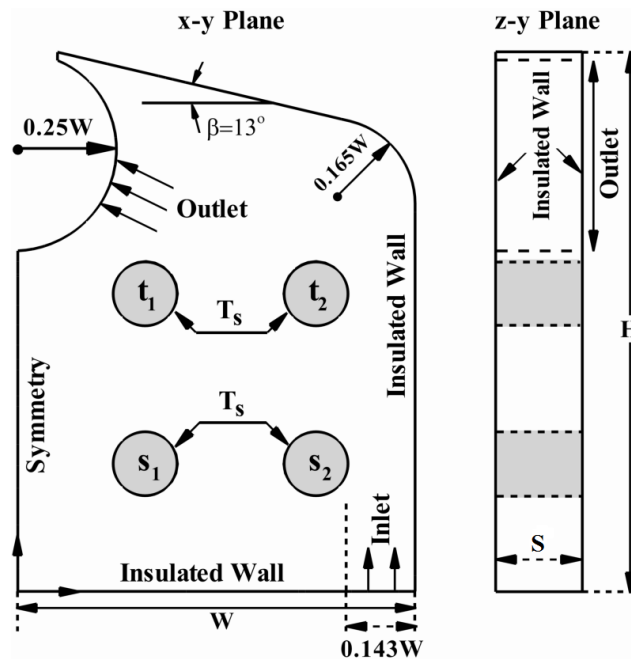


Figure3. Physical flow domain applied in this study

The governing equations of the unsteady and incompressible flow are as follows;

$$\frac{\partial u}{\partial x} + \frac{\partial v}{\partial y} + \frac{\partial w}{\partial z} = 0 \quad (1)$$

$$\frac{\partial u}{\partial \tau} + u \frac{\partial u}{\partial x} + v \frac{\partial u}{\partial y} + w \frac{\partial u}{\partial z} = -\frac{1}{\rho} \frac{\partial p}{\partial x} + \nu \left(\frac{\partial^2 u}{\partial x^2} + \frac{\partial^2 u}{\partial y^2} + \frac{\partial^2 u}{\partial z^2} \right) \quad (2)$$

$$\frac{\partial v}{\partial \tau} + u \frac{\partial v}{\partial x} + v \frac{\partial v}{\partial y} + w \frac{\partial v}{\partial z} = -\frac{1}{\rho} \frac{\partial p}{\partial y} + \nu \left(\frac{\partial^2 v}{\partial x^2} + \frac{\partial^2 v}{\partial y^2} + \frac{\partial^2 v}{\partial z^2} \right) \quad (3)$$

$$\frac{\partial w}{\partial \tau} + u \frac{\partial w}{\partial x} + v \frac{\partial w}{\partial y} + w \frac{\partial w}{\partial z} = -\frac{1}{\rho} \frac{\partial p}{\partial z} + \nu \left(\frac{\partial^2 w}{\partial x^2} + \frac{\partial^2 w}{\partial y^2} + \frac{\partial^2 w}{\partial z^2} \right) \quad (4)$$

$$\frac{\partial T}{\partial \tau} + u \frac{\partial T}{\partial x} + v \frac{\partial T}{\partial y} + w \frac{\partial T}{\partial z} = \frac{k}{\rho c_p} \left(\frac{\partial^2 T}{\partial x^2} + \frac{\partial^2 T}{\partial y^2} + \frac{\partial^2 T}{\partial z^2} \right) \quad (5)$$

The convective terms of the momentum and energy equations are discretized using the second-order upwind scheme and a second order accurate discretization is adapted to all temporal derivatives. The SIMPLE [17] algorithm is used for velocity-pressure fields coupling. The discretized equations are solved implicitly by means of the finite volume method. The convergence criteria for all flow quantities is set to 10^{-8} . The applied boundary conditions in computing the discretized governing equations are as follows;

- At lower wall

$$u = v = w = 0$$

$$\frac{\partial T}{\partial y} = 0 \quad (6)$$

- At upper wall

$$u = v = w = 0$$

$$\frac{\partial T}{\partial y} = 0 \quad (7)$$

- At right wall

$$u = v = w = 0$$

$$\frac{\partial T}{\partial x} = 0 \quad (8)$$

- At left boundary

$$\frac{\partial u}{\partial x} = \frac{\partial v}{\partial x} = \frac{\partial w}{\partial x} = 0$$

$$\frac{\partial T}{\partial x} = 0 \quad (9)$$

- At front and back walls

$$u = v = w = 0$$

$$\frac{\partial T}{\partial z} = 0 \quad (10)$$

- At inlet section

$$u = 0, v = v_{in}, w = 0$$

$$T = T_{in} \quad (11)$$

- At outlet section

$$p_{gage} = 0$$

$$(12)$$

- At the surface of hot gas passages

$$u = 0, v = 0, w = 0$$

$$T = T_s \quad (13)$$

The following parameters are used in the present study;

- Local Nusselt number

Since the hydraulic diameters of the applied passages are not identical, therefore, the section thickness is used as the characteristic length in the Nusselt number computation;

$$Nu = \frac{hS}{k} \quad (14)$$

In which;

$$h = \frac{q''}{T_s - T_{in}} \quad (15)$$

- Non-dimensional temperature

$$\theta = \frac{T - T_{in}}{T_s - T_{in}} \quad (16)$$

- Non-dimensional pressure drop

$$\Delta p^* = \frac{P_{out} - P_{in}}{\rho v_{in}^2} \quad (17)$$

Nomenclature

Parameter	Description
c_p	Specific heat
Di	Gap space between the cylinders (applicable only for validation study)
h	Heat transfer coefficient
H	Section total height
k	Conductivity
m	Water flow rate
Nu	Nusselt number
P	Pressure
P	Hot gas periphery
Δp^*	Non-dimensional pressure drop
q	Total heat transfer rate
q''	Heat flux
Re	Reynolds number
S	Section thickness
S	Second pass
T	Temperature
t	Third pass
u	Horizontal velocity
v	Vertical velocity
v	Velocity magnitude
V	Volume flow rate
w	Transverse velocity
W	Section total length
x	Horizontal coordinate
y	Vertical coordinate
z	Transverse coordinate
<i>Greek symbols</i>	
θ	Non-dimensional temperature
ν	Kinematic viscosity
ρ	Density
β	Slop of the upper wall
τ	Time
<i>Subscripts</i>	
in	inlet
out	outlet
s	Hot gas passage surface

In the present study, in order to show the effects of the hot gas passages shape on the heat and fluid flow within the section of the CIB, several shapes are considered for the cross-section of the hot gas passages such as the circle (case-1), hexagon (case-2), square (case-3), vertical ellipse (AR=2) (case-4), and horizontal ellipse (AR=2) (case-5). Figure 4 presents a general view of all under consideration cases in this investigation. All considered passages have identical peripheries as indicated in table 1. Computations are performed at two water flow rates of 0.015 and 0.030 kg/s, respectively corresponding to the Reynolds number of 373 and 746 based on the section thickness and incoming water velocity.

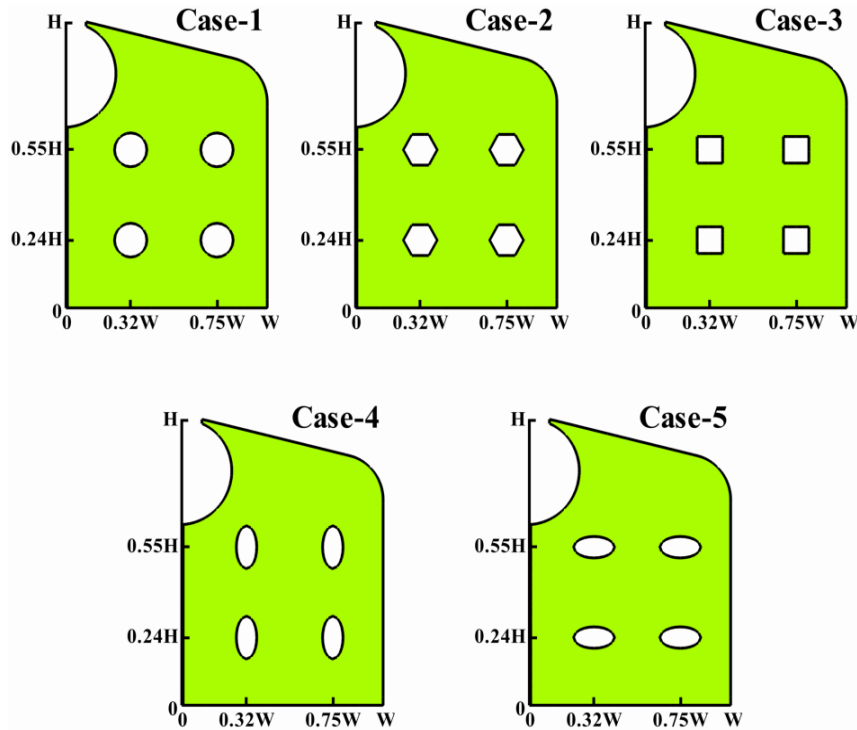


Figure4. Five cases under consideration in this study; case-1: circular passages; case-2: hexagonal passages; case-3: square passages; case-4: vertical elliptic passages with AR=2; case-5: horizontal elliptic passages with AR=2

Table1. The flow domain dimensions

Item	Dimension
Maximum height of the section	H (=1.357W)
Maximum width of the section	W
Section thickness	S(=0.285W)
Water inlet section	0.143W
Water outlet section radius	0.25W
Hot gas passage periphery (P)	0.5W

3. GRID SIZE INDEPENDENCE STUDY AND VALIDATION

The grid size independence study is an inherent process in the numerical simulations in order to find a proper grid size. In this study, several grid resolutions have been carried out to find the independent results from the grid number. It is worth mentioning that at all cases, the unstructured grids are applied within the physical domain in which the element sizes near the hot passages are minimum and by getting away from these passages, the element sizes grow gradually using a specific size function. Table 2 presents a sample of the grid test results in the section equipped with the circular passages (case-1) at two mass flow rates under consideration. As demonstrated, the values of the non-dimensional temperature at the outlet of the section do not alter after the second grid system with 45643 grids. Therefore, the corresponding element sizes are applied within all cases under consideration. Regarding the validation of the results, the applied code is validated against the available data in the literature [18]. Table 3 shows the validation results of the time-averaged Nusselt numbers at several Reynolds numbers. The comparison demonstrates the sufficient accuracy of the applied code in the present study.

Table2. Grid size independence of the section equipped with the circular passages

Grid No.	Grid Number	$\dot{m}=0.015$ kg/s		$\dot{m}=0.030$ kg/s	
		θ	Error (%)	θ	Error (%)
1	35120	0.27	---	0.25	---
2	45643	0.26	-0.74	0.24	-2.77
3	63692	0.26	-0.37	0.24	0.41
4	89930	0.26	0.37	0.24	0.41

Table3. Comparison between the mean Nusselt number and literature data for two heated circular cylinders in a square enclosure at $Re=50, 100, 150$ and 200

Re	Di=0.1		Di=0.2		Di=0.3	
	Present study	Ref. [18]	Present study	Ref. [18]	Present study	Ref. [18]
50	-	-	2.61	2.62	-	-
100	2.22	2.23	3.39	3.40	4.26	4.27
150	-	-	3.62	3.67	-	-
200	-	-	4.20	4.05	-	-

4. RESULTS AND DISCUSSION

In this section, before addressing the thermal performance of the sections under consideration, it is useful dealing with the flow structure within the section. Figure 5 demonstrates the time-averaged flow patterns within the sections under consideration. In order to show the effects of the water flow rate in the flow topology inside the section, the results are illustrated at two water flow rates of 0.015 kg/s (first row) and 0.030 kg/s (second row). At the water flow rate of 0.015 kg/s, the flow structures of circle, hexagon, and square cases are very similar to each other in terms of the number, location, and size of the developed vortical structures. Despite the first three cases, in the case of the vertical ellipse, a core vortex which develops between the hot gas passages, is considerably larger and the vortical structure between the second pass passages is extended toward the lower wall of the section. In the last case, namely horizontal ellipse, it seems the developed vortical structure on the lower wall is extended and occupied the whole region between the lower wall and second pass passages. Increasing the water flow rate up to 0.030 kg/s reveals the sensitivity of the cases to the water flow rate. As seen in figure 5, the first and last cases, namely circle and horizontal ellipse, experience the minimum changes of the flow structure in comparison to the other cases. In the highly sensitive cases such as the hexagon and square, more or less, the core vortex is eliminated at $\dot{m}=0.030$ kg/s and in the case of the vertical ellipse, the core vortex is deformed considerably and the vortical structure which had been developed between the second pass passages at 0.015 kg/s, is collapsed at 0.030 kg/s.

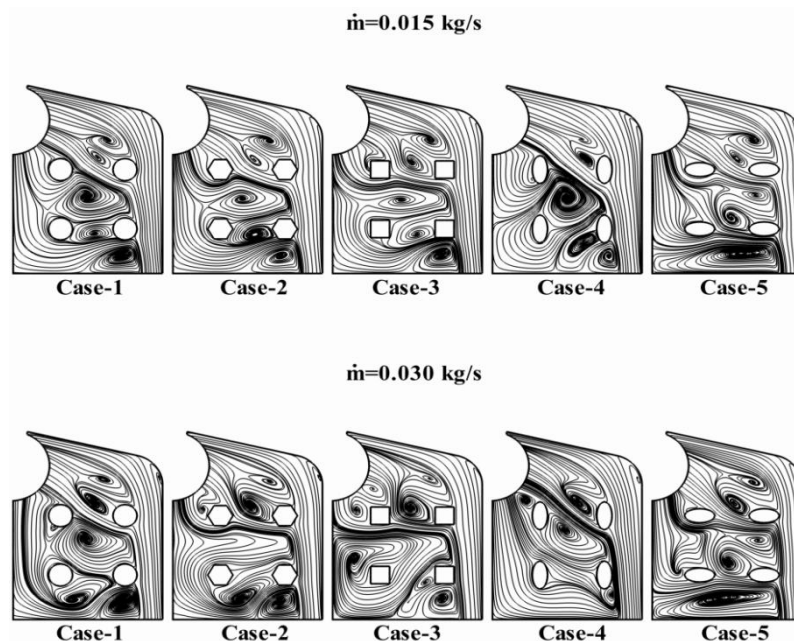


Figure5. Time-averaged flow patterns within the all sections under consideration in $\dot{m}=0.015$ kg/s (first row) and $\dot{m}=0.030$ kg/s (second row)

Figure 6 illustrates the time-averaged velocity distributions within the sections at two different water flow rates such as 0.015 kg/s (first row) and 0.030 kg/s (second row). The velocity magnitudes are normalized using the incoming velocity. It is known that interaction level of the incoming flow with hot gas passages is quite important in the section thermal performance. Figure 6 shows this interaction level clearly for all cases under consideration. In the first three cases of the circle, hexagon, and square, the injected flow into the section is very interactive with right-hand side passages of s_2 and t_2 . These interactions enhance the velocity magnitudes and consequently flow mixing within the section in general and at the left-hand side of the section in particular which is known as a useful occurrence. A bad situation is realizable in the vertical ellipse case in which the incoming flow has minimum interaction with all hot gas passages. Therefore, the velocity gradient in the core flow of the vertical ellipse case is minimum among the cases under consideration. In the last case of the horizontal ellipse, the interaction level between the incoming water flow and the hot gas passages reaches to the maximum level in comparison to the other cases. As a result, in terms of the velocity distribution within the section, the last scenario, namely horizontal ellipse case, is the best case among the cases under consideration.

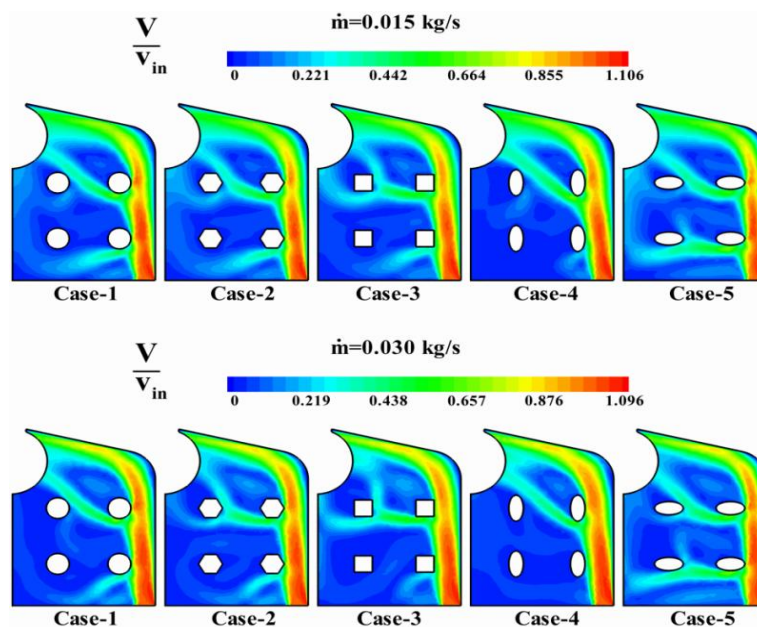


Figure6. Time-averaged non-dimensional velocity field within the all sections under consideration in $m.=0.015$ kg/s (first row) and $m.=0.030$ kg/s (second row)

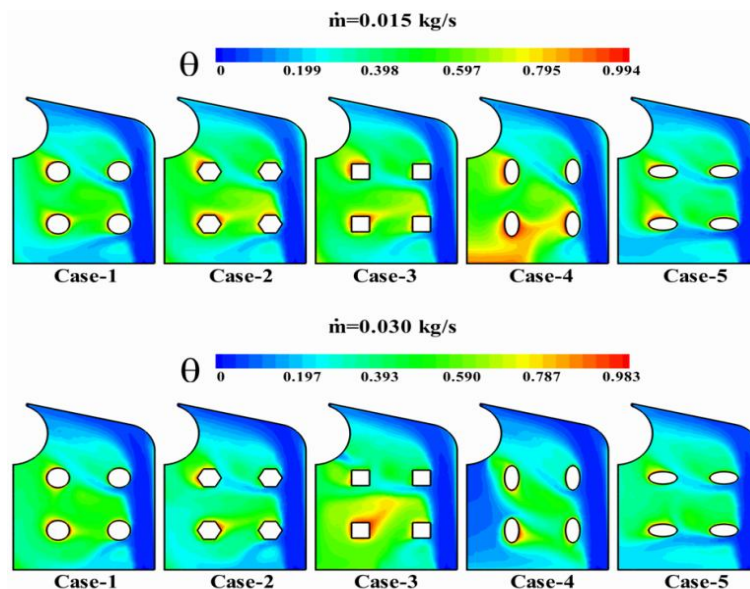


Figure7. Time-averaged non-dimensional temperature field within the all sections under consideration in $m.=0.015$ kg/s (first row) and $m.=0.030$ kg/s (second row)

Figure 7 demonstrates the non-dimensional temperature field within the all cases at 0.015 kg/s (first row) and 0.030 kg/s (second row). In general, at each individual water flow rate, the temperature gradient in the core of all sections is low due to the low-velocity magnitude in this region. The flow around the left-hand side of the hot gas passages has a low-temperature gradient regardless of the passages shape. Therefore, it is predictable that the left-hand side passages have minor contributions in the total heat transfer of the section comparing to the right-hand side. At the water flow rate of 0.015 kg/s, it seems this situation is critical for vertical ellipse case since the temperature gradient diminishes around the s_1 , s_2 , and t_1 , dramatically. Increasing the injected water flow rate up to 0.030 kg/s, although improves this bad situation in the vertical ellipse case, but provides particularly a negative result in the square case as shown in figure 7.

For enhanced visualization and in order to reveal the contribution of each hot gas passage in the total heat transfer rate of the section, the mean values of the Nusselt number of the hot gas passages are presented in figure 8 at water flow rates of the 0.015 and 0.030 kg/s. In terms of the hot gas channel id, inside the first four cases, s_1 has a minimum role in the heat transfer of the section at both water flow rates. In addition, in case-1 and case-3, the heat exchange rate of s_1 is not sensitive to water flow rate, demonstrating the unchanged velocity gradient around this channel with water injecting rate. Regarding the s_2 , as expected, case-4 has a minimum Nusselt number among the cases due to minimum interaction with the injected water flow. An interesting result occurs in case-5 in which the rates of the heat transfer of s_1 and s_2 are comparable with each other showing the considerable momentum transfer at the half-lower side of the under consideration section. Regarding t_1 and t_2 , it is clearly seen that in all sections, these two channels are the main contributors in the total heat transfer rate of the sections. The highest sensitivity of both t_1 and t_2 Nusselt numbers to the water flow rate are also seen in case-5 as illustrated in figure 8. As a result, regardless of the hot gas passage shape type, the momentum transfer and consequently the rate of the heat transfer are higher in the half-upper side of the sections in comparison to the half-lower side.

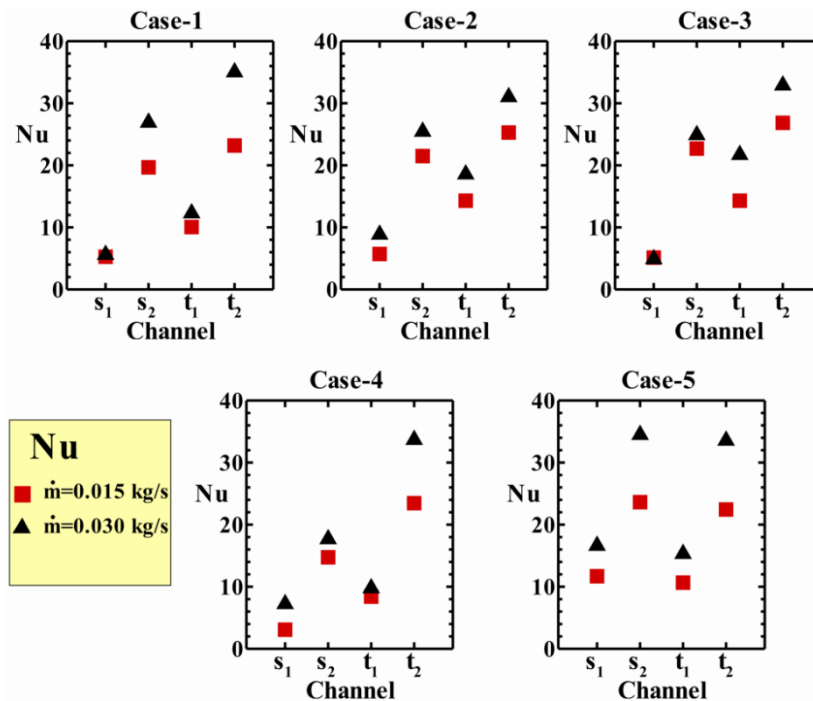


Figure8. Time-averaged mean Nusselt number of all passages in $m.=0.015$ and 0.030 kg/s

Figure 9 compares the non-dimensional total heat transfer rate of the cases at two water flow rates of 0.015 and 0.030 kg/s. It should be said that the total heat transfer rate is normalized with respect the channel thickness and thermal conductivity. As seen, at a low mass flow rate of 0.015 kg/s, the thermal performance of case-2, case-3, and case-5 are very close to each other having the higher thermal performances in comparison to the other cases. However, with an increase in the mass flow rate up to 0.030 kg/s, the section equipped with horizontal elliptic passages (case-5) provides considerably higher thermal performance compared with the other cases. On the other hand, the

section equipped with the vertical elliptic passages has the minimum heat transfer rate regardless of the water flow rate. As a result, in terms of the maximum heat transfer rate, the section equipped with the horizontal elliptic passages should be preferred among the cases under consideration.

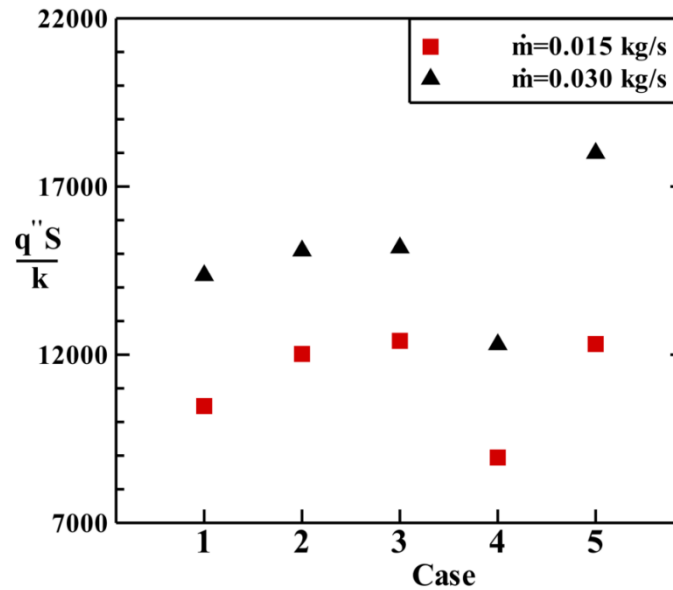


Figure9. Comparison of the non-dimensional total heat transfer rate of all passages in $\dot{m}=0.015$ and 0.030 kg/s

Although in a boiler designer, having the maximum heat transfer rate is important, having the low-pressure drop in the boiler is also a great goal. Therefore, consideration of the pressure drop occurred in the section is necessary. Figure 10 illustrates the non-dimensional pressure drop in the all sections under consideration at two different water flow rates of 0.015 and 0.030 kg/s. It is clearly seen that at each specific water flow rate, the values of the pressure drops are not considerably different among the cases. However, the sections equipped with the vertical and horizontal ellipse have minimum and maximum pressure drop among the cases under consideration, respectively. Increasing the water flow rate up to 0.030 kg/s diminishes the non-dimensional pressure drop, but the obtained trend is similar to that of the 0.015 kg/s.

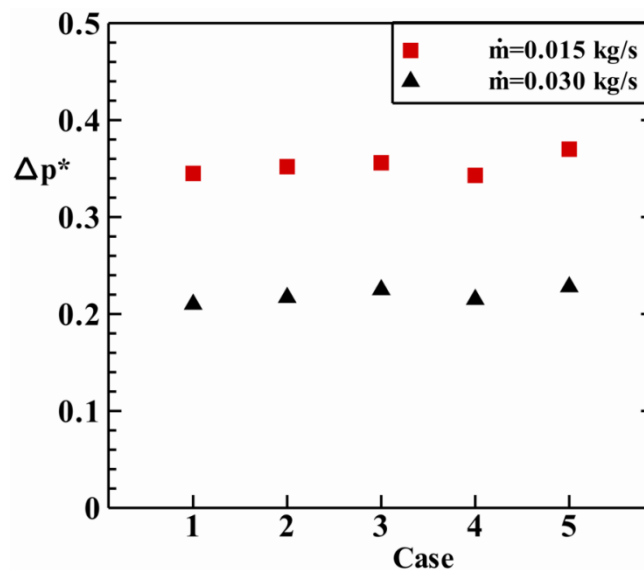


Figure10. Comparison of the non-dimensional pressure drop of all sections under consideration in $\dot{m}=0.015$ and 0.030 kg/s

By considering the total heat transfer and pressure drop penalty of the section simultaneously, determination of the optimum section among the cases under consideration is possible. Figure 11 illustrates the distributions of the goodness factor (the rate of the non-dimensional total heat transfer per non-dimensional pressure drop of the section) for all cases in two water flow rates of 0.015 and

0.030 kg/s. The comparison of the obtained results indicates that in the low water flow rate of 0.015 kg/s, although the performance indices of case-2, case-3, and case-5 are comparable, at this low water flow rate, the performance of case-3 is maximum. At the high water flow rate of 0.030 kg/s, the last case, namely case-5 has the maximum thermal-hydraulic performance in comparison to the other cases. Regardless of the water flow rate, the section with the vertical elliptic case has the minimum goodness factor among the cases under consideration. Therefore, in low and high water flow rates, the section equipped with the square and horizontal elliptic hot gas passages should be preferred during the boiler design process, respectively.

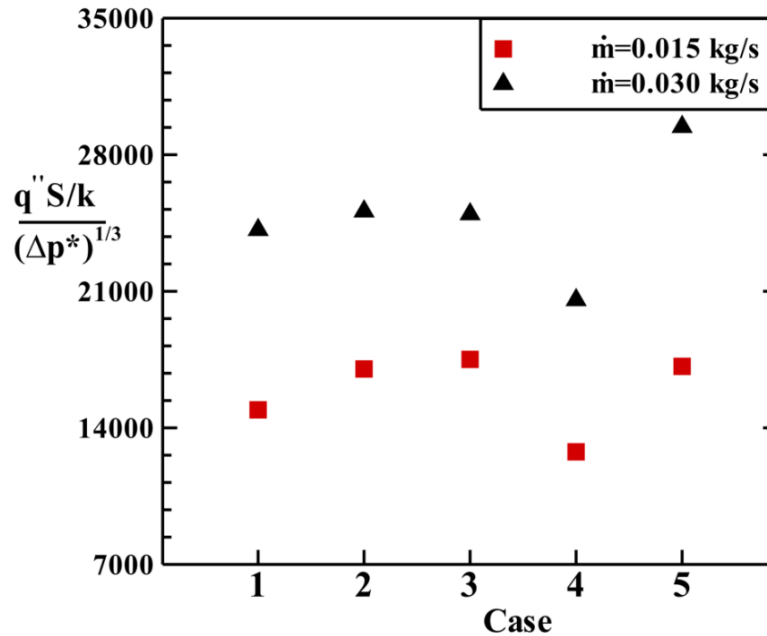


Figure 11. Distribution of the goodness factor of all sections under consideration in $\dot{m} = 0.015$ and 0.030 kg/s

5. CONCLUSION

In this numerical study, effects of the hot gas passages shape were studied three-dimensionally using the finite volume approach in two water flow rates of 0.015 and 0.030 kg/s. Various shapes were examined as the hot gas passages shape such as the circle (case-1), hexagon (case-2), square (case-3), vertical ellipse with AR= 2 (case-4), and horizontal ellipse with AR=2 (case-5) were examined to reveal the interaction level between the injected water flow and the hot gas passages. It was demonstrated that the hot gas passages which locate at the left-hand side of the section (s_1 and t_1) have a minimum role in the total heat transfer rate of the section which is one of the disadvantages of these sections from an engineering viewpoint. However, it can be said that the shape of the hot gas passages has a significant impact on the interaction level with the injected water into the section and heat exchange rate as the consequence of this interaction. In addition, it was illustrated that among the cases under consideration, sections equipped with the square and horizontal elliptic passages (case-3 and case-5) have the maximum heat transfer rate and goodness factor at water flow rates of 0.015 and 0.030 kg/s, respectively.

REFERENCES

- [1] “BP Statistical Review of World Energy,” June, 2016.
- [2] Leysens G, Trouvé G, Caplain I, Schönnenbeck C and Cazier F 2014 Energetic performances and environmental impact of the combustion of cardboard/sawdust in a domestic boiler. *Fuel*, 122: 21–27
- [3] Garcia-Maraver A, Zamorano M, Fernandes U, Rabaçal M and Costa M 2014 Relationship between fuel quality and gaseous and particulate matter emissions in a domestic pellet-fired boiler. *Fuel*, 119:141–152
- [4] Fernandes U, Guerrero M, Millera Á, Bilbao R, Alzueta M U and Costa M 2013 Oxidation behavior of particulate matter sampled from the combustion zone of a domestic pellet-fired boiler. *Fuel Process. Technol.*, 116: 201–208
- [5] Dias J, Costa M and Azevedo J L T 2004 Test of a small domestic boiler using different pellets. *Biomass Bioenergy*, 27: 531–539

- [6] Fernandes U and Costa M 2012 Particle emissions from a domestic pellets-fired boiler. *Fuel Process. Technol.*, 103:51–56
- [7] Rabaçal M Fernandes U and Costa M 2013 Combustion and emission characteristics of a domestic boiler fired with pellets of pine, industrial wood wastes and peach stones. *Renew. Energy*, 51: 220–226
- [8] Horak J Kubonova L Krpec K Hopan F Kubesa P Motyka O Laciok V Dej M Ochodek T and Placha D 2017 PAH emissions from old and new types of domestic hot water boilers. *Environ. Pollut.*, 225: 31–39
- [9] De Paepe M T'Joens C Huisseune H Van Belleghem M and Kessen V 2013 Comparison of different testing methods for gas fired domestic boiler efficiency determination. *Appl. Therm. Eng.*, 50: 275–281
- [10] Buczyński R Weber R and Szlęka A 2015 Innovative design solutions for small-scale domestic boilers: Combustion improvements using a CFD-based mathematical model. *J. Energy Inst.*, 88: 53–63
- [11] Vignali G 2017 Environmental assessment of domestic boilers: A comparison of condensing and traditional technology using life cycle assessment methodology. *J. Clean. Prod.*, vol. 142: 2493–2508
- [12] Keppel A Finnan J Rice B Owende P and MacDonnell K 2013 Cereal grain combustion in domestic boilers. *Biosyst. Eng.*, 115: 136–143
- [13] Gómez M A Porteiro J De la Cuesta D Patiño D and Míguez J L 2017 Dynamic simulation of a biomass domestic boiler under thermally thick considerations. *Energy Convers. Manage.*, 140: 260–272
- [14] Las-Heras-Casas J López-Ochoa L M Paredes-Sánchez J P 2018 Implementation of biomass boilers for heating and domestic hot water in multi-family buildings in Spain: Energy, environmental, and economic assessment. *J. Cleaner Prod.*, 176: 590–603
- [15] Hassanzadeh R Pirdavari P and Akbari Rendi M 2017 Effects of hot gas passages on the performance of multi-pass cast-iron sectional boilers. *Appl. Therm. Eng.*, 122: 171–180
- [16] Hassanzadeh R Marami Mashoof F and Darvishyadegari M 2017 Three-dimensional study on the heat transfer process in cast-iron sectional boilers. doi: 10.1007/s13369-017-2996-y
- [17] Patankar S V 1980 Numerical Heat transfer and Fluid Flow, Taylor & Francis, New York
- [18] Karimi F Xu H Wang Z Yang M and Zhang Y 2015 Numerical simulation of steady mixed convection around two heated circular cylinders in a square enclosure. *Heat Transfer Eng.*, 37: 64–75

Citation: Rahim Hassanzadeh, et.al. (2018) "A Comparative Three-Dimensional Study about the Effects of the Hot Gas Passages on a Sectional Cast-Iron Boiler Performance", *International Journal of Modern Studies in Mechanical Engineering*, 4(4), pp. 47-59. DOI: <http://dx.doi.org/10.20431/2454-9711.0404006>

Copyright: © 2018 Authors, This is an open-access article distributed under the terms of the Creative Commons Attribution License, which permits unrestricted use, distribution, and reproduction in any medium, provided the original author and source are credited.